Published in final edited form as:
NMR Biomed. 2012 February ; 25(2): 379–388. doi:10.1002/nbm.1764.

Metabolic Consequences of Treatment with the AKT Inhibitor Perifosine in Breast Cancer Cells

Judy S. Su, **Sarah M. Woods**, and **Sabrina M. Ronen**
Department of Radiology and Biomedical Imaging, University of California at San Francisco, San Francisco, California

Abstract

Activation of the PI3K/Akt pathway is associated with the development of numerous human cancers. Thus, many emerging therapies target this pathway. Previous studies have shown that targeting the PI3K/Akt pathway at the level of PI3K is associated with a drop in phosphocholine **(PCho)** and a reduction in hyperpolarized lactate production. However, the consequences of targeting downstream of PI3K at the level of Akt have not been investigated. Perifosine is an anticancer alkylphospholipid in clinical trials. It acts by inhibiting phosphorylation of Akt and was also shown to inhibit CTP:phosphocholine cytidyltransferase (CT). The goal of this study was to identify the MRS-detectable metabolic consequences of treatment with perifosine in MCF-7 breast cancer cells. We found that perifosine treatment led to a 51±5% drop in **PCho** from 30±5 fmol/cell to 15±1 fmol/cell and a comparable drop in *de novo* synthesized **PCho.** This was associated with a drop in choline kinase (ChoK) activity and ChoKα expression. CT inhibition could not be ruled out but likely did not contribute to the change in **PCho**. We also found that intracellular lactate levels decreased from 2.7±0.5 fmol/cell to 1.5±0.3 fmol/cell and extracellular lactate levels dropped by a similar extent. These findings were consistent with a drop in lactate dehydrogenase expression, and associated with a drop in activity of the hypoxia inducible factor (HIF)-1α. The drops in **PCho** and lactate production following perifosine treatment are therefore mediated downstream of Akt by the drop in HIF-1α, which serves as the transcription factor for both ChoK and lactate dehydrogenase. The metabolic changes were confirmed in a second breast cancer cell line, MDA-MB-231. Taken together, our findings indicate that **PCho** and lactate can serve as noninvasive metabolic biomarkers for monitoring the effects of inhibitors that target the PI3K/Akt pathway, independent of the step that leads to inhibition of HIF-1α.

Keywords

Magnetic resonance spectroscopy (MRS); perifosine; PI3K/Akt signaling; choline metabolism; breast cancer

INTRODUCTION

Phosphatidylinositol 3-kinases (PI3Ks) are a family of lipid kinases that catalyze the formation of phosphatidylinositol 3, 4, 5-triphosphate, which then recruits to the membrane a subset of signaling proteins with pleckstrin homology (PH) domains, including protein kinase 1 (PDK 1) and Akt (protein kinase B) (1, 2). The recruitment of these specific proteins leads to activation of downstream signaling pathways that mediate many key cellular processes including growth, proliferation, survival, and metabolism (3). The PI3K/

Corresponding author: Sabrina M. Ronen Box 2532, 1700 4th St, San Francisco Ca. 94158. sabrina.ronen@ucsf.edu Phone: 415 514 4839..

Akt pathway plays an important role in cancer biology and its activation has been associated with the development of many human cancers (4, 5). Accordingly, this signaling pathway is an attractive target for cancer therapeutics and many agents have been developed for its inhibition (6-8).

Because inhibition of the PI3K/Akt pathway is frequently associated with tumor stasis rather than tumor shrinkage, identifying biomarkers of target inhibition has been desirable both for drug development and for longitudinal monitoring of patient response. In this regard, magnetic resonance spectroscopy (MRS) has recently emerged as a promising tool (9-14). Inhibiting PI3K/Akt signaling by targeting PI3K consistently leads to an MRS detectable drop in phosphocholine (**PCho**) and total choline-containing metabolite levels (tCho, comprised of choline **PCho** and glycerophosphocholine) (10-12, 14). In addition, some studies showed a drop in hyperpolarized lactate production (12,13). However, to date, the consequences of targeting downstream of PI3K, particularly at the level of Akt, have not been investigated. Importantly, depletion of Akt, together with the other client proteins of heat shock protein 90 (HSP90), results in an elevation, rather than a drop in **PCho** (15-18). The goal of this study was therefore to monitor the MR detectable metabolic consequences of treatment with the Akt inhibitor perifosine, and to assess the generality of reduced **PCho** as a biomarker of PI3K/Akt inhibition independent of the step within the PI3K/Akt pathway being inhibited.

Perifosine (4-[[hydroxy(octadecyloxy)-phosphyinyl]oxy]-1, 1-dimethyl-piperidinium, inner salt) is an anticancer alkylphospholipid currently in clinical trials (19). The anti-neoplatic effects of perifosine are likely mediated by several factors (19, 20). A possible involvement of extracellular signal-regulated kinase (ERK) signaling or c-Jun NH2-terminal kinase (JNK) signaling have been reported (21, 22). Additionally, because the structure of perifosine resembles natural lysophosphatidylcholine, the drug can interfere with the turnover and synthesis of natural phospholipids. In particular, perifosine has been shown to inhibit CTP:phosphocholine cytidyltransferase (CT), the rate-limiting enzyme for phosphatidylcholine (PtdCho) synthesis. As a result, perifosine treatment can lead to a drop in cellular PtdCho levels and subsequent apoptosis (19, 20, 23, 24). Most importantly, like other alkylphospholipids, perifosine accumulates in lipid rafts where it interacts with the PH domain of Akt kinase to prevent its membrane localization and thus inhibit Akt phosphorylation. This leads to cell cycle arrest or apoptosis (19, 20, 25, 26). Consistent with this mechanism of action, a recent functional proteomics study demonstrated a strong correlation between perifosine-induced inhibition of Akt and the degree of perifosine antitumor efficacy in breast, ovarian, and prostate cancer cells (27).

In this study, we used multinuclear MRS and complementary biochemical assays to evaluate changes in metabolite levels and various associated enzymes in order to monitor the effect of perifosine on the metabolism of MCF-7 human breast cancer cells. We found that perifosine treatment led to a drop in total cellular **PCho** levels and a drop in lactate production. These two metabolic consequences of perifosine treatment are likely due to the observed blockade of PI3K/Akt signaling and the resulting drop in levels of the hypoxia inducible factor (HIF)-1α. Moreover, we confirmed the metabolic changes in a second breast cancer cell line, MDA-MB-231. Thus, our findings indicate that the drop in **PCho** and lactate can serve as biomarkers of PI3K/Akt signal inhibition independent of the specific target being inhibited.

MATERIALS AND METHODS

Cell Culture

MCF-7 and MDA-MB-231 human breast cancer cells were cultured in DMEM (UCSF Cell Culture Facility, San Francisco, CA) supplemented with 10% heat-inactivated fetal bovine serum (Thermo Scientific Hyclone, Logan, UT), 2 mmol/L L-glutamine (Invitrogen, Carlsbad, CA), 100 units/mL penicillin, and 100 mg/mL streptomycin (UCSF Cell Culture Facility, San Francisco, CA), at 37 °C in 5% CO_2. Both cell lines were treated with 30 μM perifosine (Cayman Europe, Estonia) (treated cells) or with ethanol at 0.06% (v/v; carrier-treated control cells) for 48 h and medium was replenished every 24 h. The concentration and exposure time of perifosine used were determined using the WST-1 cell proliferation reagent (Roche, Basel, Switzerland) to achieve ~50% drop in cell number.

In short-term labeling experiments, choline and glucose in the medium of MCF-7 cells were replaced with labeled metabolites at their normal concentrations: 28.6 μmol/L [1, 2-^{13}C] choline and 5.6 mM [1-^{13}C] glucose (Cambridge Isotope Laboratories, Inc., Andover, MA) for the last 6 h of treatment. The short-term labeling with ^{13}C-labled metabolic precursors allowed us to look at *de novo* synthesis of **PCho** and lactate production. In long-term labeling experiments, cells were incubated in medium where both choline and glucose were replaced with labeled metabolites as above for the full duration of the 48 h perifosine treatment. This allowed us to look at *de novo* synthesis of PtdCho, glycerophosphocholine (**GPCho**), fatty acids as well as glucose uptake and lactate production.

Western Blot Analysis

After 48 h treatment with perifosine or ethanol (carrier), MCF-7 cells were lysed in cell lysis buffer (Cell Signaling Technology Inc., Danvers, MA) supplemented with 1 mM phenylmethylsulfonyl fluoride (PMSF) and 1 μL/mL protease inhibitor cocktail set III (Calbiochem, Darmstadt, Germany). Lysates were incubated on ice for 10 minutes and centrifuged at 14,000 rpm for 10 min at 4 °C. The protein supernatant was collected and total protein concentrations were quantified using the Bradford assay (Bio-Rad Laboratories, Hercules, CA). Proteins were separated by SDS-PAGE using 4-20% gradient gel (Bio-Rad Laboratories, Hercules, CA) and transferred electrophoretically to nitrocellulose membranes (Millipore, Billerica, MA). Membranes were blocked in blocking buffer containing 5% nonfat dry milk in Tris-Buffered Saline Tween-20 (TBST) for an hour and incubated with primary antibodies overnight at 4 °C. The primary antibodies probed for were: Akt, P-Akt, 4E-BP1, P-4E-BP1 (obtained from Cell Signaling Technology Inc., Danvers MA), and carbonic anhydrase 9 (CAIX) (obtained from Abchem, Cambridge, MA). The membranes were then incubated with secondary antibody anti-IgG horseradish peroxidase-linked antibody (Cell Signaling Technology Inc., Danvers, MA). The proteins of interest were visualized using ECL Western Blotting Substrate (Thermo Scientific Pierce, Logan, UT).

Cell Cycle Analysis and Cell Size Determination

Samples for cell cycle analysis were prepared as previously described (28, 29). 1×10^6 cells were harvested with PBS buffer (without calcium and magnesium) (UCSF Cell Culture Facility, San Francisco, CA) and fixed with 70% ethanol (Fisher Scientifics, Pittsburgh, PA) for 24 h at 4°C. Cells were then treated with 20 μg/ml RNase A (Qiagen Inc., Valencia, CA) for 30 minutes and stained with 20 μg/ml propidium iodide (MP Biomedicals, LLC, Francs) for DNA content. Cell cycle distribution was determined using FACScan cell sorter (BD Biosciences, San Jose, CA). The cell cycle profiles were processed using the CELLQUEST and MODFIT LT software. The mean forward scatter height (FSC-H, which is a measure of relative cell size) of the G1 phase cells was also determined for the control and treated MCF-7 cells (30). In addition, cell size was determined by Beckman Coulter Multisizer III

(Beckman Coulter, Inc., Brea, CA). For this, 100 μl cell samples containing at least 1×10^6 cells were added to 10 ml of isotonic dilution solution and analyzed. The data were displayed as histograms of cell counts against cell diameters, and mean cell diameter was determined using the cell coulter software.

Cell Extraction

$4 - 5 \times 10^7$ cells were extracted using the dual-phase extraction method (29, 31). Briefly, cells were trypsinized, washed with ice-cold 0.85% saline (UCSF Cell Culture Facility, San Francisco, CA), and 10 mL ice-cold methanol (Sigma-Aldrich, St. Louis, MO) was added to the cell pellet. The solution was then subjected to: vortexing, addition of 10mL chloroform (Acros Organics, Geel, Belgium), vortexing, addition of 10mL ice cold Milli-Q water and a final vortexing. Phase separation was achieved by centrifuging the mixture at 4,400 rpm for 30 minutes at 4 °C. The aqueous and organic phases were separated and solvents were removed.

MRS Acquisition and Analysis

To acquire ^{1}H and ^{13}C spectra, the aqueous fraction was reconstituted in 400 μl deuterium oxide (Cambridge Isotope Laboratories, Inc., Andover, MA) and the lipid fraction was reconstituted in 400 μl deuterated chloroform (Acros Organics, Geel, Belgium). To acquire aqueous ^{31}P spectra, 8 μl of 500 mM ethylenediaminetetraacetic acid (EDTA) (pH 8.0) (Sigma-Aldrich, St. Louis, MO) was further added to a final concentration of 10 mM EDTA, and then the final pH was adjusted to 8.2. For lipid ^{31}P MR measurements, 200 μl of 40 mM methanolic EDTA was added to the lipid fraction that was already reconstituted in 400 μl deuterated chloroform. 40 mM methanolic EDTA was prepared by adjusting 200 mM EDTA in water to pH 6.0 with caesium hydroxide (CsOH) (Sigma-Aldrich, St. Louis, MO) and then diluted fivefold with methanol (Sigma-Aldrich, St. Louis, MO). To evaluate glucose uptake and lactate production, 500 μl of extracellular medium samples were also collected, mixed with 50 μl deuterium oxide for lock, and then directly analyzed by ^{13}C MRS.

^{1}H, ^{13}C, and ^{31}P MR spectra of the aqueous metabolite fraction, lipid metabolite fraction, and extracellular medium samples were recorded on a 600MHz INOVA spectrometer (Varian, Inc., Palo Alto, CA) using a 90° flip angle and 3 sec relaxation delay for ^{1}H, and 30° flip angle and 3 sec relaxation delay with proton decoupling for ^{13}C and ^{31}P. Fully relaxed ^{13}C, ^{31}P and ^{1}H spectra were collected in order to determine the saturation correction factor for each metabolite of interest. The concentrations of metabolites were determined by integration, correction for saturation, and normalization to cell number and to an external reference of known concentration. 2, 2, 3, 3-tetradeutero-3-trimethylsilylpropionic acid (TSP) (Cambridge Isotope Laboratories, Inc., Andover, MA) was used for ^{1}H and ^{13}C reference. Methylenediphosphonic acid (MDPA) (Sigma-Aldrich, St. Louis, MO) was used for ^{31}P reference. The perifosine peak was identified by spiking the lipid fraction with perifosine dissolved in deuterated chloroform and confirming an increase in peak intensity in the ^{31}P spectrum.

Choline Kinase (ChoK) Activity Assay

Choline kinase (ChoK) activity was determined as described previously (32). After incubation with perifosine or ethanol for 48 h, at least 1×10^7 MCF-7 cells were trypsinized, washed in ice-cold 0.85% saline, and lysed on ice in 550 μl Tris-HCl (pH 8.0) (Invitrogen, Carlsbad, CA) containing 10 mM dithiothreitol (DTT) (Acros Organics, Geel, Belgium) and 1 mM EDTA (Ambion, Austin, TX) in deuterium oxide. Cells were homogenized by passing through a fine-tipped needle (27.5 G) and then disrupted at 0 °C by sonication for 10 periods of 1s. Cell lysate was centrifuged at 14,000 rpm for 30 minutes at 4 °C and the

supernatant was retained. Reaction buffer containing choline chloride, magnesium chloride ($MgCl_2$), and adenosine triphosphate (ATP) (all from Sigma-Aldrich, St. Louis, MO) in Tris-HCl buffer was added to the supernatant right before transferring the mixture to the NMR tube. The final concentrations of substrates were 5 mM choline chloride, 10 mM ATP, and 10 mM $MgCl_2$ in 50 mM Tris-HCl (pH 8.0). ChoK activity was assayed by monitoring the temporal accumulation of **PCho** using an array of ^1H spectra at 25 °C (choice of temperature based on previously described (32) in order to minimize the degradation of ATP). ^1H spectra were acquired following presaturation of the residual water using a 90° flip angle, 3 sec relaxation delay, and 64 scans. ChoK activity was determined from the straight-line fit to plots of **PCho** (fmol/cell) versus time following addition of all substrates.

Quantitative PCR Analysis

Total cellular RNA was extracted by RNeasy Mini kit (Qiagen Inc., Valencia, CA). The quantity of total RNA was determined by using a NanoDrop ND1000 fluorospectrometer (NanoDrop Technologies, Thermo Scientific, Logan, UT). Reverse transcription was performed using the QuantiTect Reverse Transcription kit (Qiagen Inc., Valencia, CA) to obtain cDNA. The quantitative PCR was performed by UCSF Genome core and expression results were normalized to the house keeping gene, 18S rRNA (18). Primers used for amplification of ChoKα, ChoKβ, LDH-A and 18S rRNA were purchased from Applied Biosystems as Taqman Gene Expression Assays (ChoKα ID: Hs00608045_m1, ChoKβ ID: Hs00193219_m1, LDH-A ID: Hs00855332_g1, and 18S rRNA ID: Hs99999901_s1).

CTP:choline-phosphate Cytidylyltransferase (CT) Activity Assay

The CT activity was determined by a modified MRS-based method that was described in a recent study (18). In brief, about 1×10^7 MCF-7 cells were lysed on ice in 500 μL lysis buffer containing 50 mM 3-(N-morpholino)propanesulfonic acid-potassium hydroxide (MOPS-KOH) (pH 7.6), 5.5 mM sodium bisulfite (both from Sigma-Aldrich, St. Louis, MA), 1 mM PMSF (Thermo Scientific, Logan, UT), 5 mM EDTA (pH 8.0), and 5 mM ethylene glycol tetraacetic acid (EGTA) (pH 8.0) (Boston BioProducts, Ashland, MA). Cells were homogenized by passing through a fine-tipped needle (27.5 G) and then disrupted at 0 °C by sonication for 10 periods of 1 s. Cell lysate was centrifuged at 14,000 rpm for 30 minutes at 4 °C and the supernatant was retained. Reaction buffer containing **PCho** chloride, $MgCl_2$, cytidine triphosphate (CTP) (Sigma-Aldrich, St. Louis, MA), and DTT in Tris-HCl buffer was added to the supernatant right before MRS measurement. The final concentrations were 5 mM **PCho** chloride, 5 mM DTT, 10 mM CTP, 25 mM $MgCl_2$. ^{31}P decoupled spectra were collected at 33°C using a 30° flip angle, 3 second relaxation delay, and 128 scans per FID. Peak areas were integrated and concentrations were determined using the external reference, 10 mM MDPA, and further normalized to cell numbers. Concentration values of cytidine diphosphate (CDP)-choline peak were plotted against time. CT activity was determined from the straight-line fit to plots of CDP-choline (fmol/cell) versus time.

Phospholipase Activity Assays

Phospholipase A1 and A2 activity assay kits were purchased from Invitrogen (Carlsbad, California) and used following the manufacturer's instruction (18).

GPCho-Phosphodiesterase (PD) activity assay

PD activity was measured as described by Iorio et al (33). Briefly, $1 – 1.5 \times 10^7$ cells were trypsinized, washed with ice-cold 0.85% saline solution and lysed in 550 μl Tris-HCl (pH 8.0) containing 10 mM DTT and 1 mM EDTA in deuterium oxide. The reaction buffer containing L-α-glycerophosphorylcholine (Sigma-Aldrich, St. Louis, MO) and $MgCl_2$ was

added to the cell lysate right before MRS measurement. The final concentration of **GPCho** was 5 mM and that of $MgCl_2$ was 10 mM, pH 7.2. PD activity was assayed by monitoring the temporal accumulation of choline by an array of ^{1}H spectra at 28 °C using the same conditions as above. PD activity was determined from straight-line fit to plots of choline (fmol/cell) versus time.

Statistical Analysis

Results are presented as mean ± S.D. Two-tailed, unpaired Student's t-test was used to assess the statistical significance of results. P value ≤ 0.05 was considered significant.

RESULTS

Perifosine leads to inhibition of PI3K/Akt signaling associated with cell cycle arrest

MCF-7 cells were treated for 48 hours with 30 μM perifosine; a dose determined to cause a 50% drop in cell number based on the WST-1 cell proliferation assay. Following treatment, blockade of the PI3K/Akt signaling pathway was confirmed by western blot analysis (Figure 1A) which demonstrated a reduction in the levels of P-Akt and P-4E-BP1 downstream of Akt and mTOR. In addition, a drop in the levels of CAIX was observed, indicating a drop in its transcription factor HIF-1α which is also downstream of PI3K and Akt.

The effect of perifosine on cell size and cell cycle distribution was also evaluated. There was no difference in cell diameters, 19.9 ± 4.6 μm for control and 20.2 ± 4.7 μm for treated cells (n = 3, p = 0.16), and consistent with this finding there was no change in FSC-H between control and treated cells (Figure 1B). Cell cycle analysis indicated an increase in the G1 phase population, from 42 ± 6% to 70 ± 3 % (n = 4, p = 0.001), and a decrease in S phase fraction, from 45 ± 9% to 18 ± 2% (n = 4, p = 0.008), when comparing control and treated cells (Figure 1C), which is consistent with the drop in cell proliferation.

Perifosine leads to significant changes in choline phospholipid metabolism

First we investigated the effects of perifosine treatment on choline metabolism by using ^{1}H and ^{31}P MRS to monitor total metabolite levels in cell extracts of control and perifosine-treated MCF-7 cells. Our findings are summarized in Table 1. Analysis of the ^{31}P MR spectrum (Figure 2A) showed a 51 ± 5% drop in total **PCho** levels, from 30 ± 5 fmol/cell to 15 ± 1 fmol/cell (n = 4, p = 0.005), while total **GPCho** levels remained essentially unchanged at 7 ± 2 fmol/cell for control cells and at 7 ± 1 fmol/cell for treated cells (n = 4, p = 0.83). ^{1}H MRS data were consistent with these findings and indicated that total **PCho** levels decreased to 55 ± 4% (n = 4, p = 0.003) of control, whereas total **GPCho** remained constant (96 ± 24% of control; n = 4, p = 0.8). tCho levels decreased to 65 ± 5% (n = 4, p = 0.004) relative to control (Table 1). Total cellular PtdCho levels dropped slightly from 29 ± 5 fmol/cell to 23 ± 3 fmol/cell but did not reach statistical significance (n = 4, p = 0.08). In addition, 7 ± 1 fmol/cell of perifosine was detected in the ^{31}P spectra of the lipid soluble fraction of treated cells (Figure 2B).

To assess the underlying mechanism for the modulation in total **PCho** levels, we next used ^{13}C MRS and monitored short-term (6 h) 1, 2 -^{13}C-labeled choline metabolism to **PCho** by investigating the aqueous fraction of cell extracts. A significant drop was detected in ^{13}C labeled **PCho**, from 6 ± 2 fmol/cell to 3 ± 1 fmol/cell (n = 4, p = 0.02). A 60 ± 11% decrease in ^{13}C labeled betaine was also observed (Figure 2C).

Since the drop in total **PCho** levels was comparable with the drop in *de novo* ^{13}C-labeled **PCho** synthesis, we hypothesized that the drop in **PCho** was likely due to reduced synthesis of **PCho** rather than an increase in utilization. To test this hypothesis, we measured the

activity of the enzyme responsible for **PCho** synthesis, namely choline kinase (ChoK), in both control and treated MCF-7 cells using the MRS-based ChoK activity assay described previously (32). The rate of **PCho** build-up, a measure of ChoK activity, was **0.20 ± 0.01 fmol**/cell/min for control cells. After 48 h of perifosine treatment, the rate dropped to **0.13 ± 0.03 fmol**/cell/min (n = 4, p = 0.014) (Figure 3A). To rule out a direct interaction between perifosine and ChoK, perifosine was also added directly into extracted cell lysates and ChoK activity was monitored. The rate of **PCho** synthesis was not significantly altered (n = 3, p = 0.21) (data not shown). We next looked at mRNA levels for ChoKα and ChoKβ using quantitative PCR (Q-PCR) analysis. ChoKα mRNA expression levels decreased in perifosine treated cells to 58 ± 23% of control (n = 4, p = 0.03) whereas ChoKβ mRNA remained unchanged (105 ± 54%; n = 4, p = 0.86) (Figure 3B).

Perifosine has been found to inhibit CT activity leading to a drop in PtdCho biosynthesis and cellular PtdCho levels (24, 34). Our findings indicated a slight but not significant drop in the membrane phospholipid. To obtain a more complete picture of both anabolism and catabolism of PtdCho, we analyzed long-term (48 h) ^{13}C-labeled MCF-7 cell extracts. After 48 h of ^{13}C-labeling, the ^{13}C-labeled PtdCho pool in control cells was 9 ± 0.4 fmol/cell, which represented 38 ± 2% of the total PtdCho pool. In treated cells, the ^{13}C-labeled PtdCho pool was 10 ± 1 fmol/cell, representing 43 ± 2% of the total PtdCho pool. This indicated that perifosine treatment did not cause a statistically significant difference in the rate of PtdCho synthesis (n = 3, p = 0.6) (Figure 4A). The activity of the rate-limiting enzyme CT was also evaluated. To this end, we used MRS to determine the rate of CDP-choline accumulation in cell lysates following addition of choline and CTP (Figure 4B), using a similar approach to that used for assessing ChoK activity. The rate of CDP-choline build-up was **0.18 ± 0.07 fmol**/cell/min in control and **0.15 ± .05 fmol**/cell/min in treated cell extracts and the difference was not statistically significant (n = 3, p = 0.6) (Figure 4C). We then evaluated if there was a direct interaction between perifosine and CT by incubating extracted cell lysates with 30 μM perifosine for 10 minutes and comparing activity to extracted cell lysate incubated with carrier (ethanol). We found that the rate of CDP-choline build-up dropped from **0.27 ± 0.02 fmol**/cell/min in the carrier-incubated lysate to **0.12 ± 0.04 fmol**/cell/min in perifosine-incubated lysate (n = 3, p = 0.04) (Figure 4D).

GPCho, the breakdown product of PtdCho, was unaffected by perifosine treatment. However, ^{13}C-labeled **GPCho** produced from labeled PtdCho increased from 1.1 ± 0.2 fmol/cell to 2.4 ± 0.3 fmol/cell upon treatment (n = 3, p = 0.003). We therefore hypothesized that a faster breakdown of PtdCho to **GPCho** was the cause of the two-fold increase in ^{13}C-labeled **GPCho** levels. Since **GPCho** is produced by breakdown of PtdCho via phospholipase A2 (PLA2) and A1 (PLA1) followed by lysophospholipase, we evaluated the enzymatic activities of both phospholipases. Perifosine treatment caused a significant increase in PLA2 activity to 125 ± 9% of the control (n = 6, p = 0.01) and a slight drop in PLA1 activity to 95 ± 3% of the control (n = 4, p = 0.04). Because the total cellular **GPCho** levels remained constant, we also assessed the activity of **GPCho**-phosphodiesterase, the enzyme that converts **GPCho** back to choline. Using the MRS-based phosphodiesterase activity assay (33), we found that after 48 h of perifosine treatment, the rate of choline production, an indication of enzyme activity, increased to 134 ± 30% of the control, from **0.16 ± .02 fmol**/cell/min to **0.20 ± .01 fmol**/cell/min (n = 4, p = 0.02) (Figure 5A).

Perifosine leads to a drop in lactate production

PI3K/Akt signaling controls the expression of HIF-1α, which subsequently controls the expression of several of the enzymes involved in the glycolytic pathway (35-38). In some cases, PI3K/Akt signaling has also been reported to control fatty acid synthesis (39) and we have previously shown that **PCho** levels are reduced when fatty acid (FA) synthesis is

inhibited (29). We therefore wanted to assess the effect of perifosine on FA synthesis, glucose uptake, and lactate production. To this end we also incubated the cells with 1-^{13}C-labeled glucose. We found that perifosine had no effect on total FA levels or *de novo* FA synthesis. In contrast, the Akt inhibitor caused a drop in both intracellular and extracellular lactate levels. Intracellular lactate levels decreased from 2.7 ± 0.5 fmol/cell to 1.5 ± 0.3 fmol/cell (n = 3, p = 0.04) while extracellular lactate levels dropped from 1348 ± 427 fmol/cell to 640 ± 276 fmol/cell (n = 4, p = 0.04) at the end of short-term (6 h) ^{13}C-labeling. Glucose uptake dropped from 4426 ± 2211 fmol/cell for control to 4040 ± 1511 fmol/cell for treated cells but the drop did not reach significance due to the relatively large variability in glucose measurements. Consistent with the drop in lactate production, we also observed a 48 ± 26% (n = 4, p = 0.03) drop in the mRNA level of lactate dehydrogenase (LDH-A), the enzyme responsible for lactate production.

Perifosine also leads to a drop in **PCho**, tCho and lactate in MDA-MB-231 cells To confirm the generality of our findings, the metabolic consequences of perifosine treatment were investigated in a second breast cancer cell line, the more aggressive MDA-MB-231 cells. In line with the results in MCF-7 cells, we found that **PCho** levels dropped to 49 ± 6% (n=4, p=0.009) following treatment from 38.3 ± 9.2 fmol/cell in control cells to 19.0 ± 7.8 fmol/cell in treated. Also consistent with findings in MCF-7 cells, **GPCho** levels remained constant (102 ± 4%; n=4, p=0.09) and tCho levels dropped with treatment to 58 ± 6% (n=4, p=0.07). Finally as in the case of the MCF-7 cells, intracellular lactate levels dropped in MDA-MB-231 cells from 3.3 ± 0.9 fmol/cell in control cells to 1.8 ± 0.6 fmol/cell in perifosine treated cells (n=4, p=0.03).

DISCUSSION

The PI3K/Akt pathway is central to cancer development and is a promising target for novel anti-neoplastic therapies. We and others have previously shown that inhibiting signaling through this pathway by targeting PI3K leads to an MRS detectable drop in **PCho**, tCho and lactate levels (10-12, 14). However, to date, no studies have been performed to assess the metabolic sequelae of inhibitors that target Akt, downstream of PI3K. To assess the generality of reduced **PCho** and lactate as biomarkers for inhibition of the PI3K/Akt pathway, we therefore studied the effects of the Akt inhibitor perifosine. Additionally, since perifosine is an oral Akt inhibitor currently being tested in phase I and II clinical trials (19), a secondary goal of this study was to identify noninvasive MRS metabolic biomarkers of perifosine activity that could be used in the clinical setting to assess drug target modulation by this and other alkylphospholipid anti-cancer agents.

After treating MCF-7 cells with 30 μM perifosine for 48 h, we confirmed the molecular effect of perifosine on PI3K/Akt signaling. The reductions in P-Akt, P-4E-BP1 and CAIX demonstrate inhibition of Akt and its downstream targets mTOR and HIF-1α. We also confirmed that, in line with some previous reports, G1 cell cycle arrest was observed after perifosine treatment (40). Finally, we ruled out any changes in cell size as confounding factors associated with altered cellular metabolite levels observed following treatment. Of note is that our finding with regard to cell cycle arrest is in contrast to another study in prostate cancer cells wherein an increase in the G2/M phase and a decrease in the S and G0/G1 phases was observed following treatment with perifosine (52). This difference is likely due to the different cell types being investigated as well as the different treatment conditions.

We were able to detect perifosine in the lipid fraction of the cell extracts but because our studies involve cell extraction through homogenization of the cellular content, we cannot rule out redistribution of perifosine to the lipid phase during the extraction process.

Nonetheless, the presence of perifosine in the lipid metabolite fraction is consistent with the known mode of action for alkylphospholipid anti-cancer agents, and is in line with previous findings (24).

Using ^{31}P and ^{1}H MRS, a drop in total **PCho** and tCho levels was observed following treatment with perifosine in both MCF-7 and MDA-MB-231 cells. The drop in **PCho** was similar to previous findings in breast cancer cell lines treated with the PI3K inhibitors LY294002 and wortmannin (10). It was also in line with the drop in tCho observed *in vivo* following treatment of glioblastoma with the wortmannin analogue PX-866 (11) and in keeping with the drop in **PCho** and tCho levels detected when treating human prostate PC-3 cells with a specific class I PI3K inhibitor, PI-103 (14).

The overexpression of ChoKα has been closely associated with increased ChoK activity and elevated **PCho** levels in human cancer cell lines (42, 43). In light of these observations ChoK has emerged as a potential anti-cancer target (44, 45). The activity of ChoK is regulated via the PI3K pathway (44) and more recent studies show that ChoKα expression is regulated by HIF-1α, downstream of PI3K/Akt (46). Our studies show that perifosine leads to a drop in the transcriptional activity of HIF-1α (as illustrated by the drop in CAIX), a drop in ChoKα expression, and a drop in ChoK activity. Our results are therefore consistent with previous findings and also concur with the decrease in CHKα expression observed following inhibition of the PI3K/Akt pathway with PI-103 (14).

PI3K/Akt signaling has been reported to regulate expression of fatty acid synthase (FASN), the key enzyme controlling *de novo* synthesis of FA (47, 48). Moreover, a drop in **PCho** levels has been observed following FASN inhibition in previous studies, albeit without involvement of signaling via the PI3K/Akt pathway (29). Our results in this study showed that both total and *de novo* FA levels remained constant after Akt inhibition following perifosine treatment, similar to results obtained with the PI3K inhibitor PI-103 (14), and ruled out the involvement of FASN inhibition in modulation of **PCho**.

Previous studies show that in some cases alkylphospholipids accumulate within the cellular membranes and directly interact with CT leading to its rapid inhibition and thus a drop in PtdCho synthesis within a few hours of treatment (24, 34). In those studies, perifosine treatment also led to elevation of **PCho** and choline, in contrast to our findings. Nonetheless we wanted to assess CT activity as another factor that could affect **PCho** levels. When we investigated the effect of perifosine on cell extracts, we did not find a significant change in CT activity. On the other hand, we did observe inhibition of CT activity when adding perifosine directly to extracted cell lysates. Modulation of CT activity in the intact cell is complex, mediated by localization to the membrane, phosphorylation, and transcription (49-51). Our findings in cell extracts rule out any change in cellular CT activity through enzyme phosphorylation or expression, but cannot rule out altered CT activity as a result of enzyme relocalization to the membrane. Furthermore, our studies of extracts pre-incubated with perifosine indicate that the Akt inhibitor could directly interact with, and inhibit, CT in intact MCF-7 cells. We therefore cannot rule out some inhibitory effect of perifosine on CT. However; the fact that we observe a drop in **PCho** instead of an increase as previously reported with CT inhibition, combined with the knowledge that the drug has a similar effect on *de novo* 1, 2-^{13}C-labeled **PCho** accumulation and total **PCho** levels, leads us to conclude that the drop in **PCho** is primarily due to a drop in ChoK expression and activity. A drop in choline transport into the cell could also contribute to the drop in **PCho** and explain the fact that betaine levels also dropped. Further studies are needed to address this issue.

Following perifosine treatment, total cellular **GPCho** levels stayed constant while ^{13}C-labeled **GPCho** increased significantly. We verified that an increase in PLA2 activity was

the likely explanation for the elevated ^{13}C-labeled **GPCho** levels and that the rise in **GPCho**phosphodiesterase activity with perifosine treatment counter-balances the faster breakdown of PtdCho to **GPCho** to keep total **GPCho** levels constant. Previous studies have shown that the PI3K inhibitor wortmannin leads to elevated total **GPCho** levels while LY294002 and PI-103 do not. This possibly indicates a complex and variable interplay between the PI3K/Akt pathway, PLA2 and **GPCho**-phosphodiesterase activities.

Perifosine treatment also led to a drop in lactate production in MCF-7 and MDA-MB-231 cells in line with our previous studies showing a drop in hyperpolarized lactate production (12,13). Like the drop in ChoKα expression, this is likely due to the drop in HIF-1α activity, which is known to control LDH expression (36) and shows that the most significant metabolic changes observed in this study are mediated by the same PI3K/Akt effectors.

HSP90 inhibition, which results in depletion of multiple HSP90 client proteins including Akt, leads to an elevation rather than a drop in **PCho** (15-18). Our observation that Akt inhibition by perifosine leads to a decrease in **PCho**, rules out Akt as a factor that could mediate this elevation in **PCho**.

In summary, this study shows that the main metabolic consequences of treatment with the Akt inhibitor perifosine are a drop in **PCho** and a drop in lactate production. Both of these metabolic effects are likely mediated by the reduction in HIF-1α transcriptional activity and could serve as metabolic biomarkers of signal inhibition upstream of HIF-1α.

Acknowledgments

The authors would like to acknowledge Sarah Elmes for assistance with cell cycle analysis, Christopher Ward for development of the CT activity assay, and Srirupa Roy for advice on western blots and helpful discussion. This work was supported by National Institutes of Health grant R01 CA130819.

LIST OF ABBREVIATIONS

PI3K	phosphatidylinositol 3-kinase
PCho	phosphocholine
CT	CTP:phosphocholine cytidyltransferase
PtdCho	Phosphatidylcholine
HIF-1α	hypoxia inducible factor 1α
GPCho	glycerophosphocholine
CAIX	carbonic anhydrase 9
ChoK	choline kinase
PLA1	phospholipase A1
PLA2	phospholipase A2
PD	GPC-phosphodiesterase
FA	fatty acids

REFERENCES

1. Fresna-Vara JA, Casado E, de Castro J, Cejas P, Belda-Iniesta C, Gonzalez-Baron M. PI3K/Akt signalling pathway and cancer. Cancer Treatment Reviews. 2004; 30:193–204. [PubMed: 15023437]

2. Pawson T, Nash P. Protein-protein interaction define specificity in signal transduction. Genes & Development. 2000; 14:1027–1047. [PubMed: 10809663]

3. Engelman JA, Luo J, Cantley LC. The evolution of phosphatidylinositol 3-kinases as regulators of growth and metabolism. Nature Reviews Genetics. 2006; 7:606–619.

4. Fry MJ. Phosphoinositide 3-kinase signalling in breast cancer: how big a role might it play? Breast Cancer Research. 2001; 3:304–312. [PubMed: 11597319]

5. Vivanco I, Sawyers CL. The Phosphatidylinositol 3-Kinase-Akt Pathway in Human Cancer. Nature Reviews Cancer. 2002; 2:489–501.

6. Hennessy BT, Smith DL, Ram PT, Lu Y, Mills GB. Exploiting the PI3K/Akt pathway for cancer drug discovery. Nature Reviews Drug Discovery. 2005; 4:988–1004.

7. Courtney KD, Corcoran RB, Engelman JA. The PI3K pathway as drug target in human cancer. Journal of Clinical Oncology. 2010; 28:1075–1083. [PubMed: 20085938]

8. Engelman JA. Targeting PI3K signalling in cancer: opportunities, challenges and limitations. Nature Reviews Cancer. 2009; 9:550–562.

9. Ronen SM, Jackson LE, Beloueche M, Leach MO. Magnetic resonance detects changes in phosphocholine associated with Ras activation and inhibition in NIH 3T3 cells. Br J Cancer. 2001; 84:691–696. [PubMed: 11237392]

10. Beloueche-Babari M, Jackson LE, Al-Saffar NM, Eccles SA, Raynaud FI, Workman P, Leach MO, Ronen SM. Identification of magnetic resonance detectable metabolic changes associated with inhibition of phosphoinositide 3-kinase signaling in human breast cancer cells. Mol Cancer Ther. 2006; 5:187–196. [PubMed: 16432178]

11. Koul D, Shen R, Kim YW, Kondo Y, Lu Y, Bankson J, Ronen SM, Kirkpatrick DL, Powis G, Yung WK. Cellular and in vivo activity of a novel PI3K inhibitor, PX-866, against human glioblastoma. Neuro Oncol. 2010; 12:559–569. [PubMed: 20156803]

12. Ward CS, Venkatesh HS, Chaumeil MM, Brandes AH, Vancriekinge M, Dafni H, Sukumar S, Nelson SJ, Vigneron DB, Kurhanewicz J, James CD, Haas-Kogan DA, Ronen SM. Noninvasive detection of target modulation following phosphatidylinositol 3-kinase inhibition using hyperpolarized 13C magnetic resonance spectroscopy. Cancer Res. 2010; 70:1296–1305. [PubMed: 20145128]

13. Dafni H, Larson PE, Hu S, Yoshihara HA, Ward CS, Venkatesh HS, Wang C, Zhang X, Vigneron DB, Ronen SM. Hyperpolarized 13C spectroscopic imaging informs on hypoxiainducible factor-1 and myc activity downstream of platelet-derived growth factor receptor. Cancer Res. 2010; 70:7400–7410. [PubMed: 20858719]

14. Al-Saffar NM, Jackson LE, Raynaud FI, Clarke PA, de Molina AR, Lacal JC, Workman P, Leach MO. The phosphoinositide 3-kinase inhibitor PI-103 downregulates choline kinase a leading to phosphocholine and total choline decrease detected by magnetic resonance spectroscopy. Cancer Research. 2010; 70:5507–5517. [PubMed: 20551061]

15. Chung YL, Troy H, Banerji U, Jackson LE, Walton MI, Stubbs M, Griffiths JR, Judson IR, Leach MO, Workman P, Ronen SM. Magnetic resonance spectroscopic pharmacodynamic markers of the heat shock protein 90 inhibitor 17-allylamino,17-demethoxygeldanamycin (17AAG) in human colon cancer models. J Natl Cancer Inst. 2003; 95:1624–1633. [PubMed: 14600095]

16. Sankaranarayanapillai M, Tong WP, Yuan Q, Bankson JA, Dafni H, Bornmann WG, Soghomonyan S, Pal A, Ramirez MS, Webb D, Kaluarachchi K, Gelovani JG, Ronen SM. Monitoring histone deacetylase inhibition in vivo: noninvasive magnetic resonance spectroscopy method. Mol Imaging. 2008; 7:92–100. [PubMed: 18706291]

17. Chung YL, Troy H, Kristeleit R, Aherne W, Jackson LE, Atadja P, Griffiths JR, Judson IR, Workman P, Leach MO, Beloueche-Babari M. Noninvasive magnetic resonance spectroscopic pharmacodynamic markers of a novel histone deacetylase inhibitor, LAQ824, in human colon carcinoma cells and xenografts. Neoplasia. 2008; 10:303–313. [PubMed: 18392140]

18. Brandes AH, Ward CS, Ronen SM. 17-allyamino-17-demethoxygeldanamycin treatment results in a magnetic resonance spectroscopy-detectable elevation in choline-containing metabolites associated with increased expression of choline transporter SLC44A1 and phospholipase A2. Breast Cancer Res. 2010; 12:R84. [PubMed: 20946630]

19. Gills JJ, Dennis PA. Perifosine: update on a novel Akt inhibitor. Curr Oncol Rep. 2010; 11:102–110. [PubMed: 19216841]
20. van Blitterswijk WJ, Verheij M. Anticancer Alkylphosphospholipids: Mechanisms of Action, Cellular Sensitivity and Resistance, and Clinical Prospects. Current Pharmaceutical Design. 2008; 14:2061–2074. [PubMed: 18691116]
21. Crul M, Rosing H, de Klerk GJ, Dubbelman R, Traiser M, S. R, Knebel NG, Schellens JHM, Beijnen JH, ten Bokkel Huinink WW. Phase I and pharmacological study of daily oral administration of perifosine (D-21266) in patients with advanced solid tumours. European Journal of Cancer. 2002; 38:1615–1621. [PubMed: 12142051]
22. Elrod HA, Lin Y-D, Yue P, Wang X, Lonial S, Khuri FR, Sun S-Y. The alkylphospholipid perifosine induces apoptosis of human lung cancer cells requiring inhibition of Akt and activation of the extrinsic apoptotic pathway. Mol Cancer Ther. 2007; 6:2029–2038. [PubMed: 17604333]
23. van der Luit AH, Vink SR, Klarenbeek JB, Perrissound D, Solary E, Verheij M, van Blitterswijk WJ. A new class of anticancer alkylphospholipids uses lipid rafts as membrane gateways to induce apoptosis in lymphoma cells. Mol Cancer Ther. 2007; 6:2337–2345. [PubMed: 17699729]
24. Boggs KP, Rock CO, Jackowski S. Lysophosphatidylcholine and 1-O-octadecyl-2-O-methyl-rac-glycero-3-phosphocholine inhibit the CDP-choline pathway of phosphatidylcholine synthesis at the CTP:phosphocholine cytidylyltransferase step. J Biol Chem. 1995; 270:7757–7764. [PubMed: 7706325]
25. Kondapaka SB, Singh SS, Dasmahapatra GP, Sausville EA, Roy KK. Perifosine, a novel alkylphospholipid, inhibits protein kinase B activation. Molecular Cancer Therapeutics. 2003; 2:1093–1103. [PubMed: 14617782]
26. Ruiter GA, Zerp SF, Bartelink H, van Blitterswijk WJ, Verheij M. Anti-cancer alkyl-lysophospholipids inhibit the phosphatidylinositol 3-kinase-Akt/PKB survival pathway. Anti-Cancer Drugs. 2003; 14:167–173. [PubMed: 12569304]
27. Hennessy BT, Lu Y, Poradosu E, Yu Q, Yu S, Hall H, Carey MS, Ravoori M, Gonzalez-Angulo AM, Birch R, Henderson IC, Kundra V, Mills GB. Pharmacodynamic markers of perifosine efficacy. Clin Cancer Res. 2007; 13:7421–7431. [PubMed: 18094426]
28. Wang XW, Zhan Q, Coursen JD, Khan MA, Kontny HU, Yu L, Hollander MC, O'Connor PM, Fornace AJ Jr. Harris CC. GADD45 induction of a G2/M cell cycle checkpoint. Proc Natl Acad Sci USA. 1999; 96:3706–3711. [PubMed: 10097101]
29. Ross J, Najjar AM, Sankaranarayanapillai M, Tong WP, Kaluarachchi K, Ronen SM. Fatty acid synthase inhibition results in a magnetic resonance-detectable drop in phosphocholine. Mol Cancer Ther. 2008; 7:2556–2565. [PubMed: 18723500]
30. Fingar DC, Salama S, Tsou C, Harlow E, Blenis J. Mammalian cell size is controlled by mTOR and its downstream targets S6K1 and 4EBP1/eIF4E. Genes & Development. 2002; 16:1472–1487. [PubMed: 12080086]
31. Tyagi RK, Azrad A, Degani H, Salomon Y. Simultaneous Extraction of Cellular Lipids and Water-Soluble Metabolites: Evaluation by NMR Spectroscopy. MRM. 1996; 35:194–200.
32. Iorio E, Mezzanzanica D, Alberti P, Spadaro F, Ramoni C, D'Ascenzo S, Millimaggi D, Pavan A, Dolo V, Canevari S, Podo F. Alterations of Choline Phospholipid Metabolism in Ovarian Tumor Progression. Cancer Research. 2005; 65:9369–9376. [PubMed: 16230400]
33. Iorio E, Ricci A, Bagnoli M, Pisanu ME, Castellano G, Di Vito M, Venturini E, Glunde K, Bhujwalla ZM, Mezzanzanica D, Canevari S, Podo F. Activation of Phosphotidylcholine Cycle Enzymes in Human Epithelial Ovarian Cancer Cells. Cancer Research. 2010; 70:2126–2135. [PubMed: 20179205]
34. van der Luit AH, Budde M, Ruurs P, Verheij M, van Blitterswijk WJ. Alkyl-lysophospholipid accumulates in lipid rafts and induces apoptosis via raft-dependent endocytosis and inhibition of phosphatidylcholine synthesis. J Biol Chem. 2002; 277:39541–39547. [PubMed: 12183451]
35. Shaw RJ, Cantley LC. Ras, PI(3)K and mTOR signalling controls tumour cell growth. Nature. 2006; 441:424–430. [PubMed: 16724053]
36. Semenza GL. Targeting HIF-1 for cancer therapy. Nat Rev Cancer. 2003; 3:721–732. [PubMed: 13130303]

37. Bardos JI, Ashcroft M. Hypoxia-inducible factor-1 and oncogenic signalling. Bioessays. 2004; 26:262–269. [PubMed: 14988927]
38. Pouyssegur J, Dayan F, Mazure NM. Hypoxia signalling in cancer and approaches to enforce tumour regression. Nature. 2006; 441:437–443. [PubMed: 16724055]
39. Menendez JA, Lupu R. Fatty acid synthase and the lipogenic phenotype in cancer pathogenesis. Nat Rev Cancer. 2007; 7:763–777. [PubMed: 17882277]
40. Patel V, Lahusen T, Sy T, Sausville EA, Gutkind JS, Senderowicz AM. Perifosine, a novel alkylphospholipid, induces $p21^{WAF1}$expression in squamous carcinoma cells through a p53-independent pathway, leading to loss in cyclin-dependent kinase activity and cell cycle arrest. Cancer Research. 2002; 62:1401–1409. [PubMed: 11888912]
41. Kozma SC, Thomas G. Regulation of cell size in growth, development and human disease: PI3K, PKB and S6K. Bioessays. 2002; 24:65–71. [PubMed: 11782951]
42. Nakagami K, Uchida T, Ohwada S, Koibuchi Y, Suda Y, Sekine T, Morishita Y. Increased choline kinase activity and elevated phosphocholine levels in human colon cancer. Jpn J Cancer Res. 1999; 90:419–424. [PubMed: 10363580]
43. Ramirez de Molina A, Banez-Coronel M, Gutierrez R, Rodriguez-Gonzalez A, Olmeda D, Megias D, Lacal JC. Choline kinase activation is a critical requirement for the proliferation of primary human mammary epithelial cells and breast tumor progression. Cancer Research. 2004; 64:6732–6739. [PubMed: 15374991]
44. Ramirez de Molina A, Gutierrez R, Ramos MA, Silva JM, Silva J, Bonilla F, Sanchez JJ, Lacal JC. Increased choline kinase activity in human breast carcinomas: clinical evidence for a potential novel antitumor strategy. Oncogene. 2002; 21:4317–4322. [PubMed: 12082619]
45. Ramirez de Molina A, Sarmentero-Estrada J, Belda-Iniesta C, Taron M, ramirez de Molina V, Cejas P, Skrzypski M, Gallego-Ortega D, de Castro J, Rosell R, Gonzalez-Baron M, Lacal JC. Expression of choline kinase alpha to predict outcome in patients eith early-stage non-small-cell lung cancer: a retrospective study. The Lancet Oncology. 2007; 8:889–897. [PubMed: 17851129]
46. Glunde K, Shah T, Winnard PT, Raman V, Takagi T, Vesuna F, Artemov D, Bhujwalla ZM. Hypoxia regulates choline kinase expression through hypoxia-inducible factor-1α signaling in a human prostate cancer model. Cancer Research. 2008; 68:172–180. [PubMed: 18172309]
47. Wang HQ, Altomare DA, Skele KL, Poulikakos PI, Kuhajda FP, Di Cristofano A, Testa JR. Positive feedback regulation between AKT activation and fatty acid synthase expression in ovarian carcinoma cells. Oncogene. 2005; 24:3574–3582. [PubMed: 15806173]
48. Menendez JA, Lupu R. Fatty acid synthase and the lipogenic phenotype in cancer pathogenesis. Nature Reviews Cancer. 2007; 10:763–777.
49. Jackowski S, Fagone P. CTP: Phosphocholine cytidylyltransferase: paving the way from gene to membrane. J Biol Chem. 2005; 280:853–856. [PubMed: 15536089]
50. Kent C. CTP:phosphocholine cytidylyltransferase. Biochim Biophys Acta. 1997; 1348:79–90. [PubMed: 9370319]
51. Sugimoto H, Banchio C, Vance DE. Transcriptional regulation of phosphatidylcholine biosynthesis. Prog Lipid Res. 2008; 47:204–220. [PubMed: 18295604]
52. Floryk D, Thompson T. Perifosine induces differentiation and cell death in prostate cancer cells. Cancer Lett. 2008; 266(2):216–226. [PubMed: 18395973]

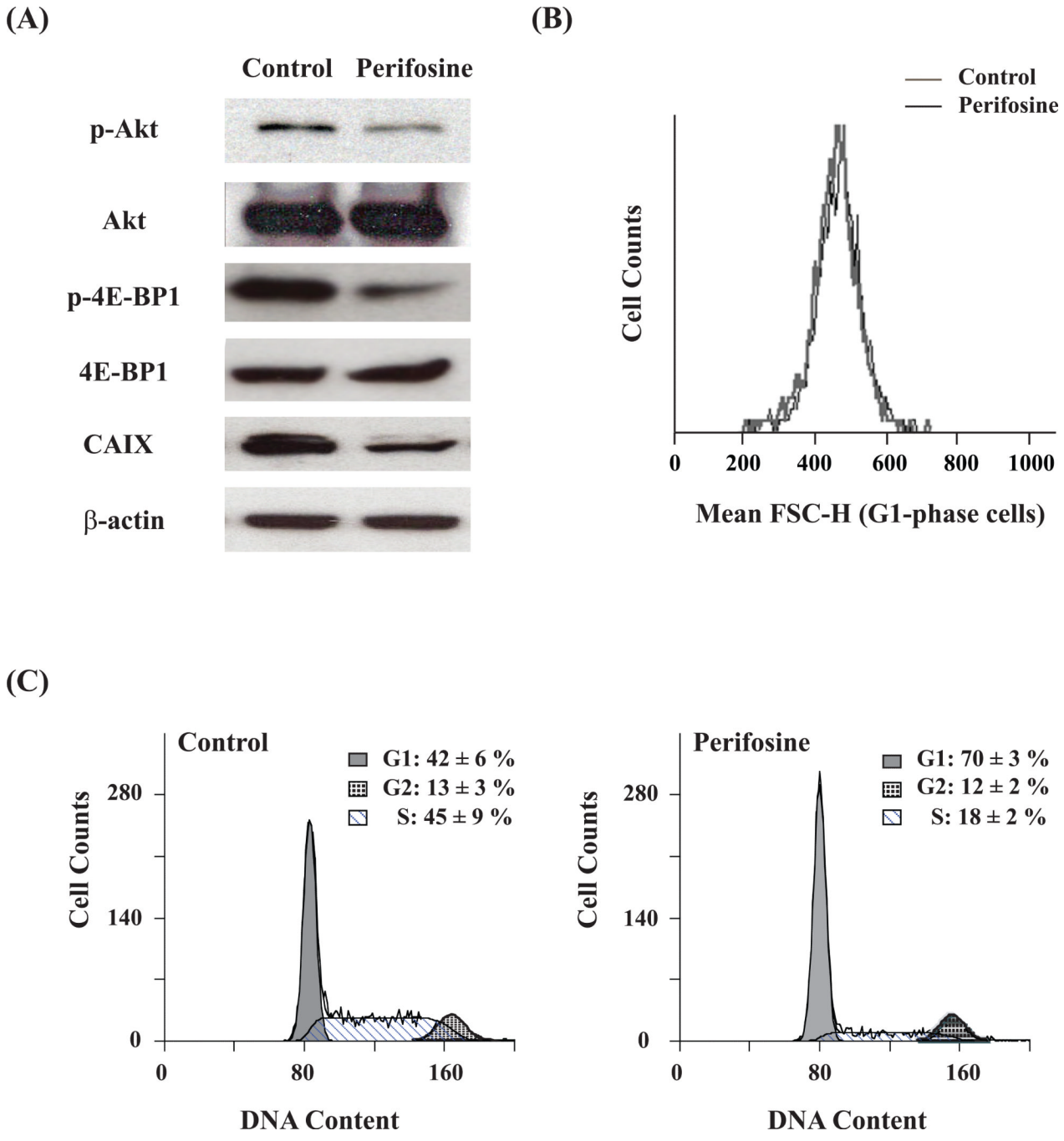

Figure 1. Biological effects of 48 h perifosine treatment on MCF-7 cells

(A) Western blot analysis of P-Akt, Akt, P-4E-BP1, 4E-BP-1, CAIX, and β-actin (loading control) showing the effect on protein expression. (B) Mean FSC-H of G1-phase cells showing the effect on cell size. (C) Cell cycle distribution showing the effect on cell cycle.

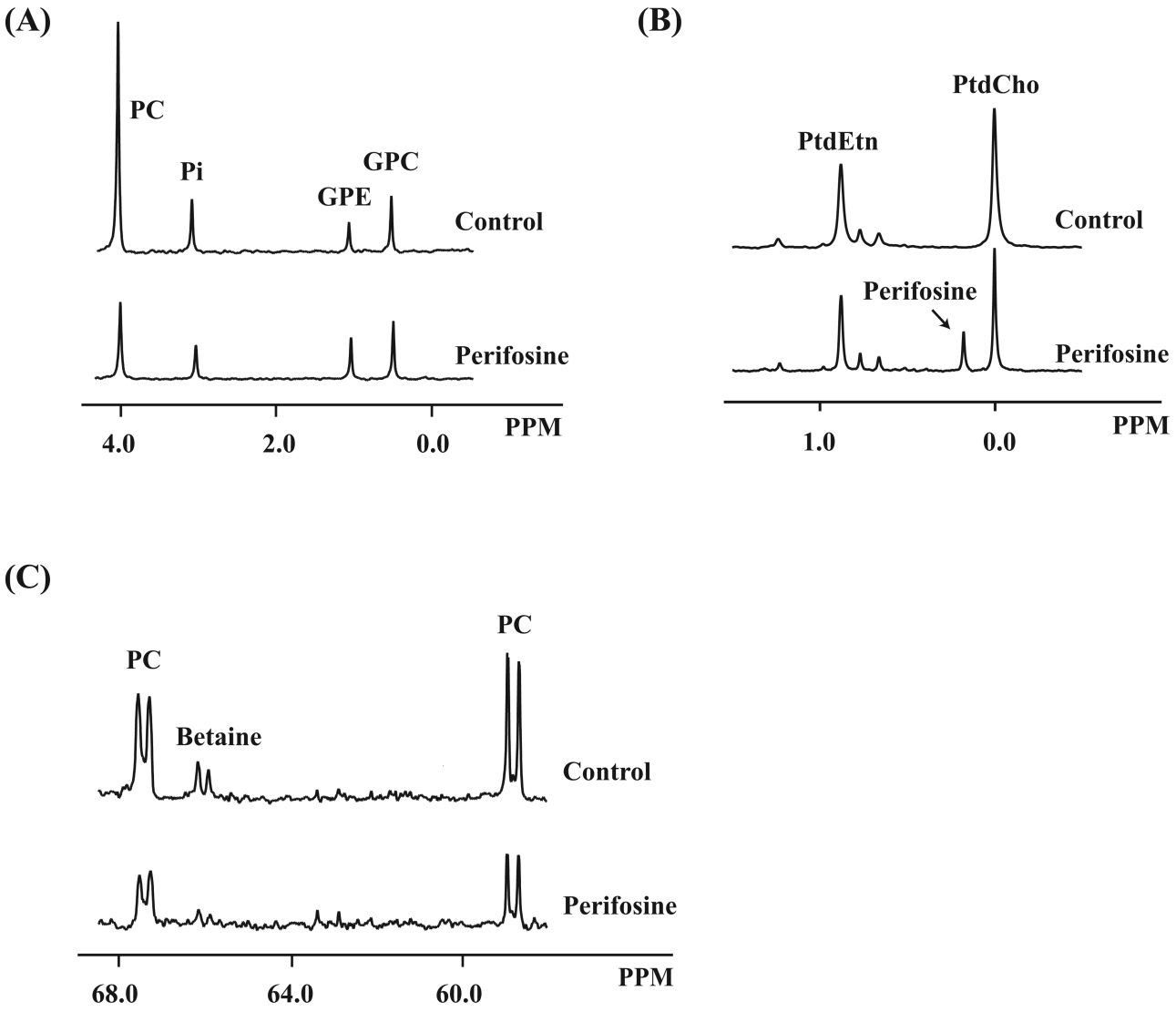

Figure 2. Effect of perifosine on MRS-detectable choline-containing metabolites in MCF-7 cell extracts

(A) Representative ^{31}P MR spectra of aqueous fraction showing the effect of treatment on total **PCho** and **GPCho** levels. (B) Representative ^{13}P MR spectra of lipid fraction showing the effect on total PtdCho levels and the accumulation of perifosine. (C) Representative ^{13}C MR spectra of aqueous fraction upon perifosine treatment on *de novo* synthesis of **PCho**.

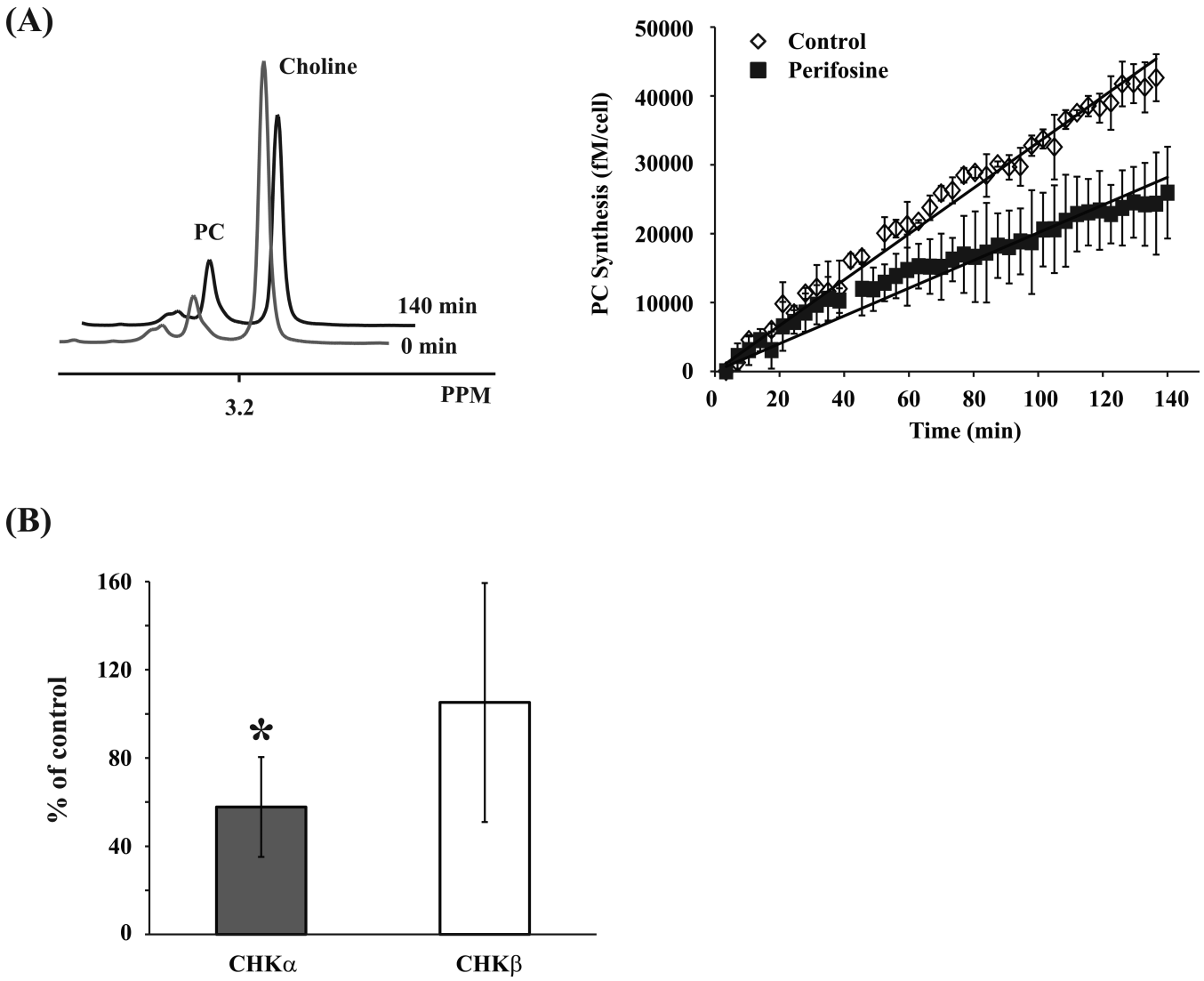

Figure 3. Effect of perifosine on ChoK

(A) Choline kinase activity: ^{1}H MR spectra of MCF-7 cell lysate at the beginning and at the end of ChoK activity assay measurement. The conversion of choline to **PCho** was monitored throughout the reaction time period. Representative plot of **PCho** biosynthesis versus time from control (◇) and treated (■) cells. The data was fit to a straight-line to obtain the rates of PC synthesis. (B) Choline kinase expression: mRNA levels of CHKα and CHKβ in treated cells expressed as % of the control from Q-PCR analysis.

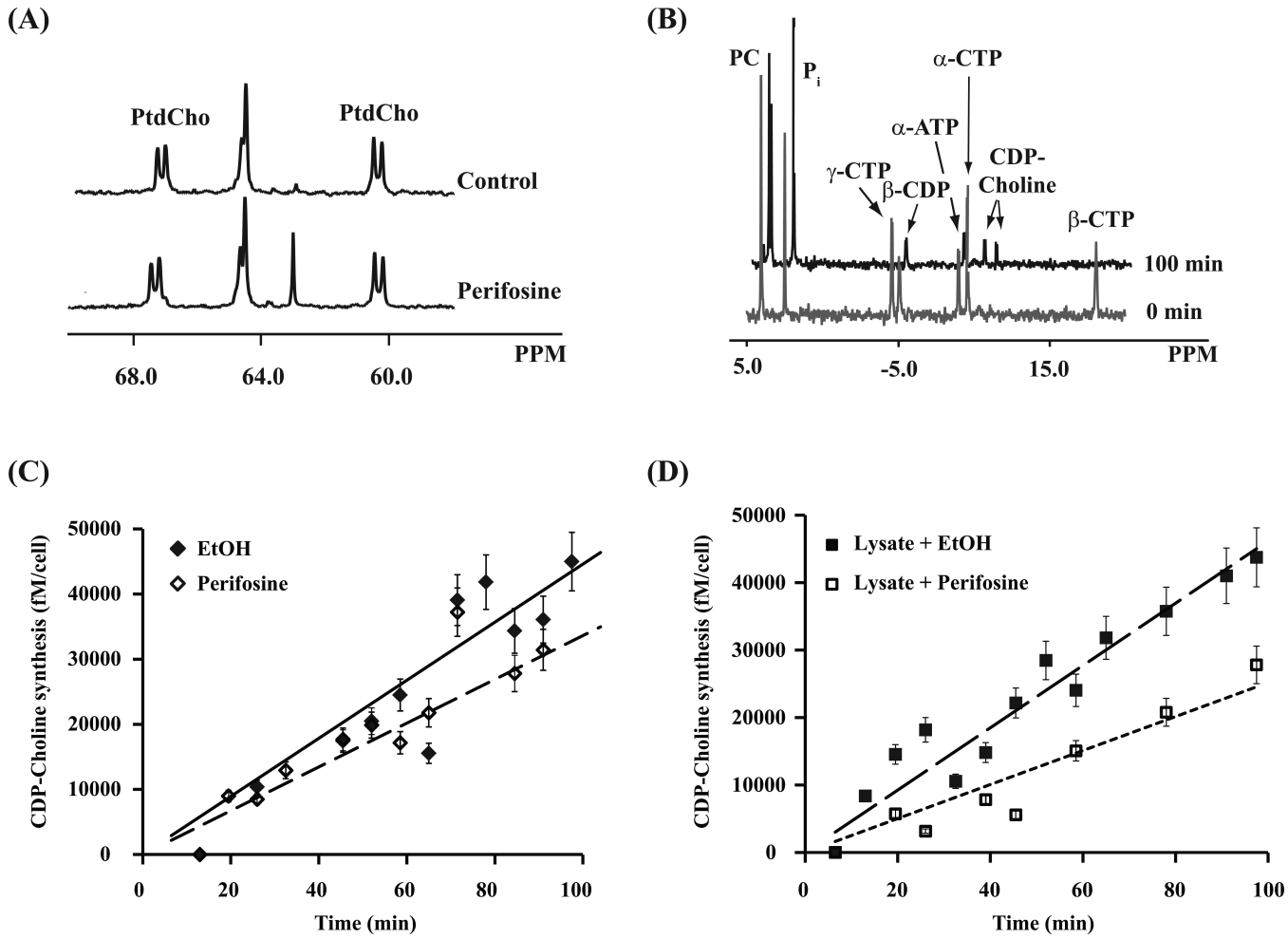

Figure 4. Effect of perifosine on CT

(A) Representative ^{13}C spectra of lipid fraction showing the effect of treatment on *de novo* synthesis of PtdCho. (B) ^{31}P spectra of MCF-7 cell lysate at the beginning and the end of CT activity assay measurement. The concentration of reaction product, CDP-Choline, was plotted against time, and the synthesis rate was determined from the slope of the straight-line fit. (C) Representative plot of CDP-Choline biosynthesis versus time in control cell lysate (◆) and perifosine-treated cell lysate (◇). (D) Representative plot of CDP-Choline biosynthesis versus time from extracted cell lysate plus EtOH (■) and extracted cell lysate plus 30 μM perifosine (□).

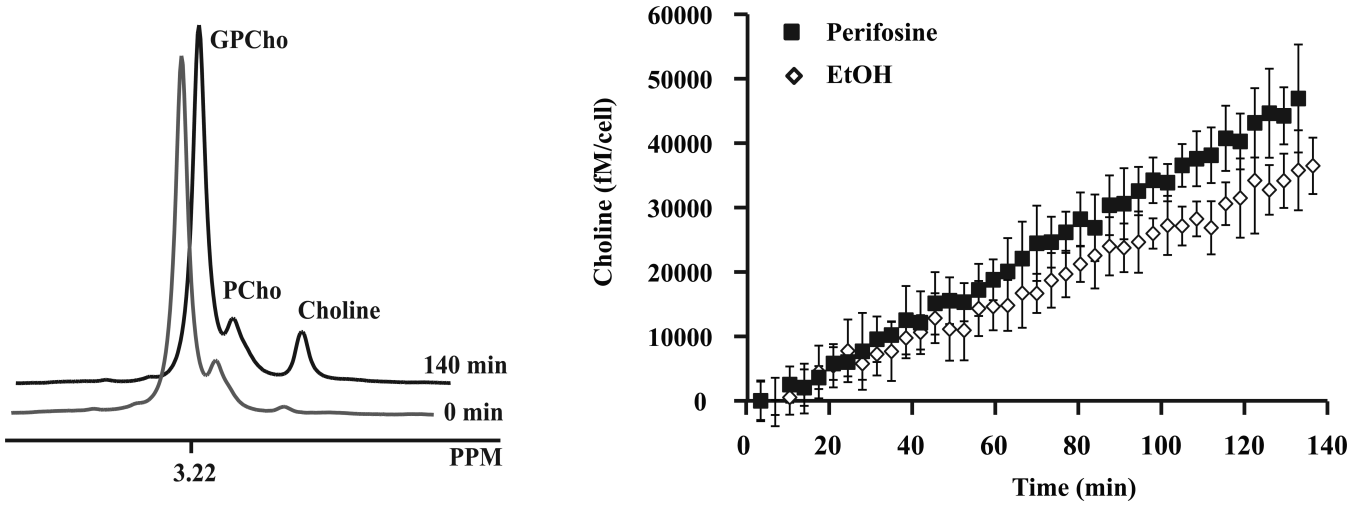

Figure 5. Effect of perifosine on GPCho-phosphodiesterase

^{1}H MR spectra of MCF-7 cell lysate at the beginning and at the end of phosphodiesterase activity assay measurement. The conversion of **GPCho** to choline was monitored throughout the reaction time period. Representative plot of choline biosynthesis versus time from both control (◇) and treated (■) cells. The data was fit to a straight-line to obtain the rates of choline formation.

Table 1

Summary of changes in metabolite levels in cancer cells with 30μM perifosine

Metabolite (fmol/cell)	EtOH	Perifosine	% of control	p-value
In MCF-7 cancer cells				
PCho (total, ^{31}P)	30±5	15±1	51±5	0.005*
PCho (total, ^{1}H)	27±5	15±4	55±4	0.003*
GPCho (total, ^{31}P)	7±2	7±1	105±18	0.8
GPCho (total, ^{1}H)	9±3	8±1	96±24	0.6
Choline (^{1}H)	2±1	2±.2	78±31	0.3
tCholine (total, ^{1}H)	38±5	25±5	65±5	0.004*
PtdCho (total, ^{31}P)	29±5	23±3	79±6	0.08
PCho** (*de novo*, ^{13}C)	6±2	3±1	51±12	0.025*
GPCho# (*de novo*, ^{13}C)	1±0.2	2±0.3	223±62	0.003*
PtdCho (*de novo*, ^{13}C)	9±0.4	10±1	104±14	0.249
Intracellular lactate (^{1}H)	2.7±0.5	1.5±0.3	48±24	0.04*
Extracellular lactate (^{13}C)	1348±427	640±276	55±33	0.04*
In MDA-MB-231 cancer cells				
PCho(total, ^{1}H)	38±9	19±8	50±8	.009*
GPCho(total, ^{1}H)	11±2	10±2	90±19	0.7
tCholine(total, ^{1}H)	52±12	29±9	55±11	0.03*
Intracellular lactate (^{1}H)	3.3±0.9	1.8±0.6	55±18	0.03*

*P<.05 (two tailed unpaired Student's t-test)

**Concentrations determined from short-term 13C labeling

#Concentrations determined from long-term ^{13}C labeling